International Journal of Applied Mathematics in Control Engineering 5 (2022) 109-113

Contents lists available at YXpublications

International Journal of Applied Mathematics in Control Engineering

Journal homepage: http://www.ijamce.com

Prediction Of Milling Cutter Wear Based on ASO-BP Neural Network

Shida Cai[a], Liangliang Sun[a,*], Mantong Zhao[b], Wang Yue[c], Xi Li[d], Jiayu Peng[e]

[a] *School of Electrical and Control Engineering, Shenyang Jianzhu University, 110168, China*

[b] *School of Economics and Management, Shenyang Institute of Technology, 113000, China*

[c] *School of Sports, Shenyang Jianzhu University, 110168, China*

[d] *School of Management, Shenyang Jianzhu University, 110168, China*

[e] *School of Mechanical Engineering, Shenyang Jianzhu University, 110168, China*

ARTICLE INFO

Article history:
Received 20 June 2022
Accepted 30 September 2022
Available online 5 October 2022

Keywords:
Prediction of milling cutter wear
Atomic search algorithm
Back propagation neural network
Forecasting model

ABSTRACT

Back Propagation Neuron Network (BPNN) is a common method for milling cutter wear prediction. However, due to the random selection of its initial weight threshold, the traditional BPNN has the problems of slow convergence speed, low prediction accuracy and easy to fall into local optimal solution in the training process. An atom search algorithm (ASO) is proposed to optimize the prediction method of the initial weight threshold of the error back propagation neural network. Firstly, the time-domain and frequency-domain feature extraction of the cutting force, vibration and acoustic emission signals of the milling cutter is carried out, and then the wavelet packet analysis (WPA) is used for the time-frequency domain feature extraction. Secondly, the prediction model of ASO-BP neural network is constructed to predict the milling cutter wear. The experimental results show that compared with the traditional BP neural network, the ASO-BP neural network model proposed in this paper has faster convergence speed and higher prediction accuracy in the prediction process of milling cutter wear.

1. Introduction

In the cutting process, the milling cutter directly contacts the machined workpiece, and its wear degree plays a decisive role in the machining quality of the workpiece. Because of the importance of milling cutter wear to milling cutter cutting process, the study of milling cutter wear prediction has been concerned by the majority of scholars(e.g., Zhang C et al.,2013). The prediction of tool wear in traditional milling process usually adopts manual experience. However, due to the low prediction accuracy of manual experience, the milling cutter will be replaced before and after reaching the blunt value(e.g., Tzab C et al.,2021). If the milling cutter is replaced before reaching the blunt standard of the milling cutter, it will cause waste of resources and increase production costs. If the milling cutter is replaced after reaching the blunt standard of the milling cutter, the wear value exceeds the expected wear, which will lead to poor quality of the workpiece that cannot meet the accuracy requirements and even lead to greater economic losses due to machine tool failure shutdown. Therefore, it is of great significance to achieve accurate prediction of milling cutter wear(e.g., Jian B L et al.,2020).

* Corresponding author.
E-mail addresses: sunliangliang@sjzu.edu.cn (L. Sun)
doi:

Milling tool wear prediction problem is mainly divided into two parts: signal extraction process and model prediction process. During the signal extraction process, Ghasempoor A demonstrated the correlation between real-time changes in cutting forces and milling cutter wear, Hesser D F successfully predicted milling cutter wear using velocity sensor signals(e.g., Ghasempoor A et al.,1999), and Wang C proposed a milling cutter wear prediction method using acoustic emission sensors(e.g., Hesser, D. F et al.,2019). In the process of model prediction, Kaya B proves the feasibility of neural network to predict the wear of milling cutter(e.g., Kaya B et al.,2011). Gomes M C successfully predicts the wear of milling cutter through support vector machine model(e.g., Gomes M C et al.,2021). Chungchoo C uses fuzzy neural network to predict. The prediction results show that the model can accurately estimate the maximum wear depth of milling cutter(e.g., Chungchoo C et al.,2002). The experimental results of Li W prove that the hidden Markov model has strong versatility for milling cutter wear(e.g., Li W et al.,2019).

In this paper, a tool wear prediction model based on atom search optimization-back propagation neural network (ASO-BP) is proposed and simulated by using the excellent nonlinear mapping

ability of error back propagation neural network (BP) and the strong clustering search ability of atom search optimization (ASO).

2. Feature extraction and fusion

2.1 Principle of Wavelet Packet Analysis

Wavelet packet transform is a more comprehensive signal processing technology evolved on the basis of wavelet transform. It improves the disadvantage of poor frequency resolution of wavelet analysis in a signal in the middle and high frequency bands, and divides the high frequency and low frequency parts at the same time. Fig. 1 shows the three-layer decomposition structure diagram of wavelet packet. S is the original signal. A and D represent the low-frequency and high-frequency components, respectively. The number is the decomposition layer (e.g., Li C B,2007).

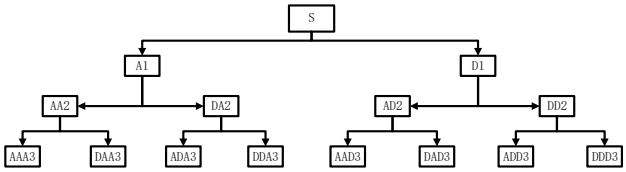

Fig. 1. Wavelet Packet Three - Layer Decomposition Structure Diagram

The expression of wavelet packet decomposition is expressed as:

$$d_l^{j,2n} = \sum_k h_{k-2l} d_k^{j+1,n} \tag{1}$$

$$d_l^{j,2n+1} = \sum_k g_{k-2l} d_k^{j+1,n} \tag{2}$$

The expression of wavelet packet reconstruction is expressed as:

$$d_l^{j+1,n} = \sum_k \left[h_{l-2k} d_k^{j,2n} + g_{l-2k} d_k^{j,2n+1} \right] \tag{3}$$

In the formula, j represents the number of decomposition layers; d represents the wavelet coefficient; g and h represent high and low pass filters respectively.

2.2 feature extraction

This paper uses the public data of PHM2010 data challenge(e.g., Li X et al.,2009), and the experimental platform diagram is shown in Figure 2.

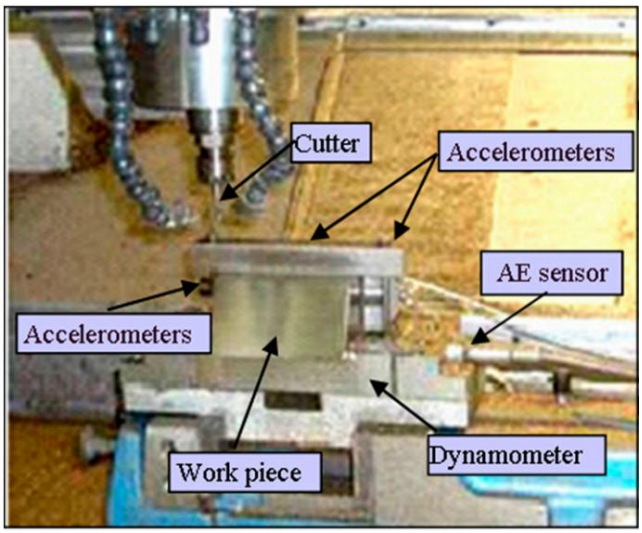

Fig. 2. schematic of experimental platform

The wear data of C1, C4 and C6 milling cutters were obtained, and the data of each milling cutter included 315 times of walking cutter data of three-dimensional cutting force signal, three-dimensional vibration signal and one acoustic emission signal.

A total of 168 features were obtained from the time domain, frequency domain feature extraction and three-layer wavelet packet analysis of 7 sensor signals in each milling cutter wear data, and Pearson correlation analysis was carried out between these features and the real wear value. As shown in Fig. 3, 17 feature values with high correlation were taken as the input of the neural network.

The calculation formula of Pearson correlation coefficient is:

$$\rho_{XY} = \frac{\sum_{i=1}^{N} (x_i - \bar{x})(y_i - \bar{y})}{\left[\sum_{i=1}^{N} (x_i - \bar{x})^2 \sum_{i=1}^{N} (y_i - \bar{y})^2 \right]^{\frac{1}{2}}} \tag{4}$$

In the formula, X is the signal eigenvalue; Y is milling cutter wear value.

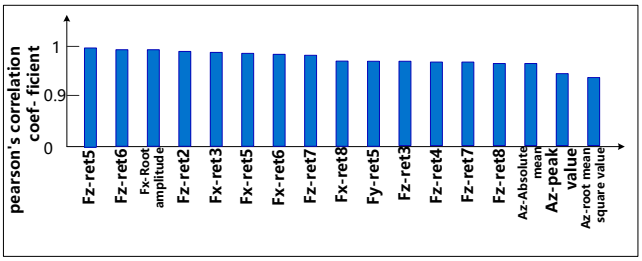

Fig. 3. Eigenvalues with high correlation

3. Principle of ASO-BP Neural Network Model

3.1 Principle of Wavelet Packet Analysis

BP neural network is a multilayer feedforward network trained by error back propagation algorithm. The weight threshold of the network is adjusted by reverse propagation to minimize the network error. BP neural network model includes input layer, hidden layer and output layer. The data are input from the input layer, and enter the hidden layer through the calculation of weights. When the threshold is reached in the hidden layer, the output of the hidden layer is obtained through the activation function, and then the output of the network is obtained through the calculation of the same principle in the output layer. This process is the forward propagation process of the network. The output results of the network are compared with the expected results, and the error generated by the comparison is used to reversely adjust the weight threshold in the neural network. This process is the error back propagation process of the neural network. Fig. 4 shows the BP neural network model(e.g.,Lv et al.,2011).

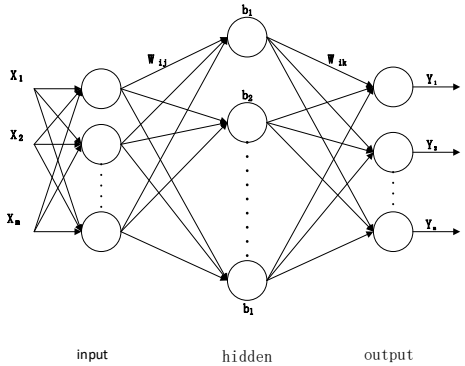

Fig. 4. BP neural network model diagram

The output of the hidden layer is:

$$H_j = g\left(\sum_{i=1}^{n} \omega_{ij} x_i + a_j\right) \tag{5}$$

In the formula: $g(x)$ is sigmoid activation function; ω_{ij} is the weight from the input layer to the hidden layer; x_i for network input; a_j is the threshold of hidden layer.

The output of the output layer is:

$$O_k = \sum_{j=1}^{l} H_j \omega_{jk} + b_k \tag{6}$$

In the formula: ω_{jk} is the weight of the hidden layer to the output layer; b_k is the threshold for the output layer.

The error is:

$$E = \frac{1}{2}\sum_{k=1}^{m} (Y_k - O_k)^2 \tag{7}$$

3.1 ASO-BP Neural Network Model

The traditional BP neural network model is easy to fall into local optimum in training because of the random definition of its initial weight threshold. In order to solve this problem, ASO is introduced to optimize the BP neural network model, which can effectively improve the accuracy of model prediction. The flow chart of ASO-BP neural network model is Fig.5.

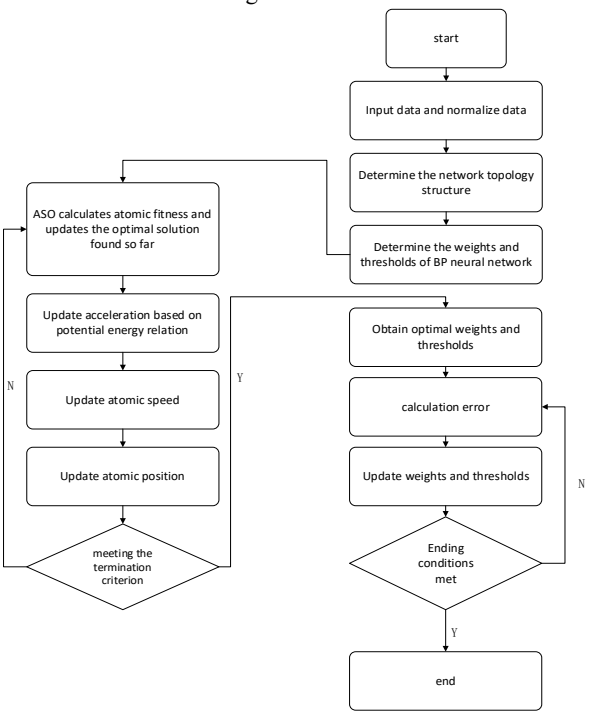

Fig. 5. Flow chart of ASO-BP neural network model

The steps of ASO-BP neural network model are:

Step 1 determines the number of hidden layers of BP neural network, the number of neurons in each layer, the initial weight threshold, the size of the atomic group, the position and speed of each atom in the initial group.

Step 2 determines the fitness function. The fitness function of ASO algorithm is set as:

$$f\left[x_i^d(t)\right] = \frac{1}{2}\sum_{p}^{m}\sum_{q}^{n}\left(\theta_j^p - O_j^p\right)^2 \tag{8}$$

In the formula: θ_q^p for the p training sample, the j output layer output neuron point of the real value, O_q^p is the predicted value ; n is the total number of training samples ; m is the number of nodes in the output layer ; $x_i^d(t)$ is the ith atom in d-dimensional space in the tth iteration of the ASO algorithm.

Step 3 Calculate the mass of each atom:

$$m_i^d(t) = \frac{M_i(t)}{\sum_{j=1}^{N} M_j(t)} \tag{9}$$

$$M_i(t) = e^{-\frac{f_i(t) - f_{\min}(t)}{f_{\max}(t) - f_{\min}(t)}} \tag{10}$$

In the formula: $m_i^d(t)$ is the quality of the ith atom in the d-dimensional space at the tth iteration, and the quality of the atom can be calculated by its function fitness. The better the function fitness is, the greater the atomic quality is; $f_i(t)$ is the fitness of the i th atom at the t th iteration, $f_{\max}(t)$ and $f_{\min}(t)$ represent the values of the maximum fitness and the minimum fitness atom at the tth iteration, respectively.

Step 4 calculates the acceleration of each atom:

$$a_i^d(t) = \frac{F_i^d(t)}{m_i^d(t)} + \frac{G_i^d(t)}{m_i^d(t)} \tag{11}$$

In the formula: $F_i^d(t)$ is the interaction force between the other atoms in the d-dimensional space at the tth iteration; $G_i^d(t)$ is the binding force of the atomic system at the tth iteration.

Step 5 Update atomic velocity and position:

$$v_i^d(t+1) = rand_i^d v_i^d(t) + a_i^d(t) \tag{12}$$

$$X_i^d(t+1) = X_i^d(t) + v_i^d(t+1) \tag{13}$$

In the formula: $rand_j^d$ is the random number in $[0,1]$.

Step 6 Repeat steps 2-6 to update the optimal atomic position until the termination condition is satisfied to output the optimal initial weight threshold.

4. Prediction examples and analysis

4.1 prediction model building

Since the input sample dimension is not high and there is no need to select too many hidden layers to reduce the network scale, the three-layer network topology is selected, and the input layer nodes are 17 eigenvalues with high correlation. The number of nodes in the output layer is one corresponding to the wear value of the milling cutter. The number of nodes in the hidden layer is usually selected according to the empirical formula. The formula is:

$$l = \sqrt{m+n} + a \tag{14}$$

In the formula: m is the number of nodes in the input layer; n is the number of nodes in the output layer; a is a constant between 1 and 10.

According to the formula, the interval of determining the number of nodes in the hidden layer can be set at $[5,14]$. The number of nodes in the interval is brought into the BP neural network for training, and

the relationship between the mean square error of the training results of the number of nodes in each hidden layer and the number of nodes is shown in Fig.6. Therefore, the number of hidden layer nodes is finally set as 11 with the smallest mean square error.

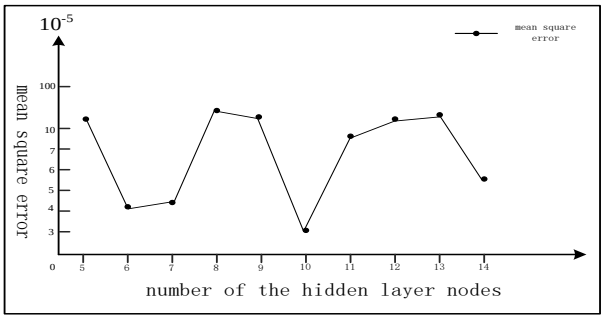

Fig. 6. Relationship between the number of hidden layer nodes and mean square error

The hidden layer node activation function is Sigmoid, and the expression is:

$$y = \frac{1}{\left(1+e^{-x}\right)} \tag{15}$$

In the formula: x, y represent the input and output of the node, respectively.

The output layer node activation function is Identity, expressed as:

$$y = x \tag{16}$$

The training objective of neural network is 10^{-5}, and BP neural network is optimized by atomic search algorithm. In the atomic search algorithm, the initial population size is 30, the maximum number of iterations is 50, the individual range is $[-3.1,3.1]$, the depth weight is 50, and the multiplier weight is 0.2.

4.2 results and analysis of precision

In the experiment, all the data in C4 are used as training set to train the neural network and select the optimal model. Using the trained neural network model, C1 and C6 are used as test sets.

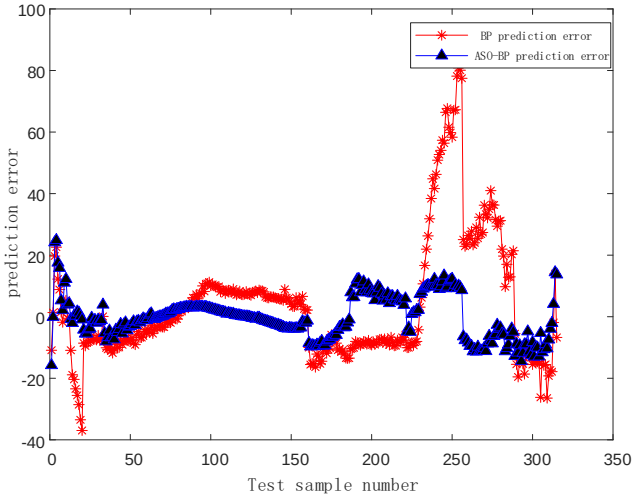

Fig. 7. Comparison of prediction error between BP and ASO-BP on tool c1

In the simulation experiment, by comparing the prediction results, it can be found that the prediction accuracy of ASO-BP neural network is significantly higher than that of the traditional BP neural network. Fig. 7 and Fig.8 shows the prediction results on the data set C1, where the average absolute percentage error MAPE of the BP neural network prediction results is 12.5 % and the average absolute error MAE is 14, and the average absolute percentage error MAPE of the ASO-BP prediction results is 5.1 % and the average absolute error MAE is 5.4.

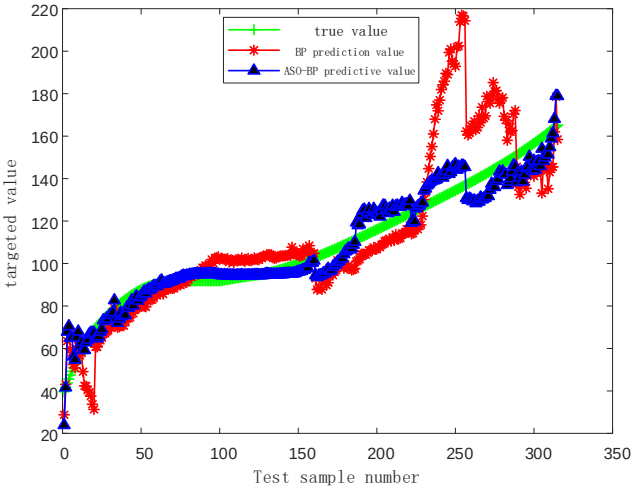

Fig. 8. Prediction results of BP and ASO-BP on tool c1

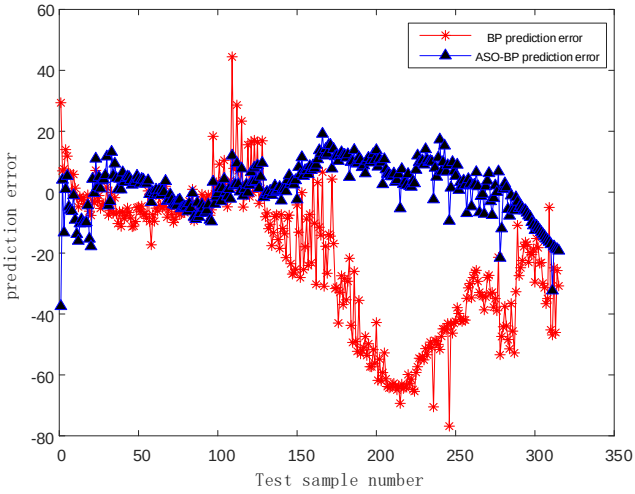

Fig. 9. Comparison of prediction error between BP and ASO-BP on tool c6

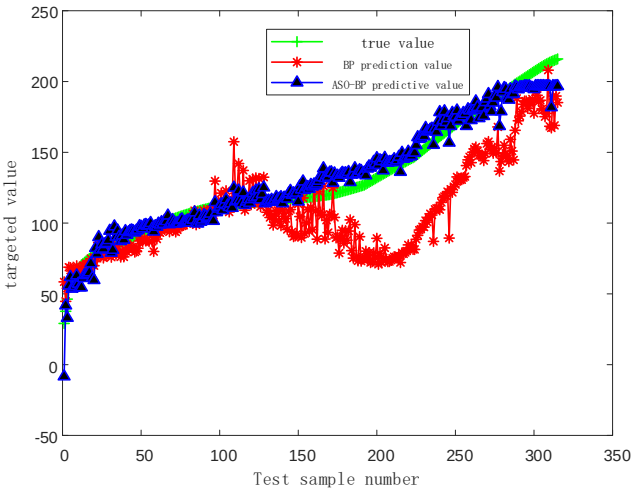

Fig. 10. Prediction results of BP and ASO-BP on tool c6

Fig. 9 and Fig.10 shows the prediction results on the data set C6, where the average absolute percentage error MAPE of the BP neural network prediction results is 17.3 % and the average absolute error MAE is 24.1, and the average absolute percentage error MAPE of the

ASO-BP prediction results is 5.6 % and the average absolute error MAE is 6.6. It can be seen that the scheme in this paper significantly improves the prediction accuracy.

5. Results

In view of the shortcomings of the traditional BP neural network that often falls into local optimal solution and slow convergence, this paper uses ASO-BP neural network to establish the prediction model of tool wear. A tool wear prediction model based on ASO-BP neural network is proposed. The interaction force and constraint force of atomic motion in nature are simulated by atomic search algorithm, and the initial weights and thresholds of BP neural network are defined to improve the state estimation accuracy of the model. The simulation results show that the prediction accuracy of ASO-BP neural network is significantly improved compared with the traditional BP neural network.

Acknowledgements

The research is sponsored by the National Natural Science Foundation of China (61873174, 61503259), Liaoning Provincial Natural Science Foundation of China (2020-KF-11-07，20180550613)

References

Zhang, C. , & Zhang, J. . (2013). On-line tool wear measurement for ball-end milling cutter based on machine vision. *Computers in Industry*, *64*(6), 708-719.

Tzab, C. , Czab, C. , Yw, D. , Xz, E. , & Thab, C. . (2021). A vision-based fusion method for defect detection of milling cutter spiral cutting edge - sciencedirect. *Measurement*, *177*.

Jian, B. L. , Yu, K. T. , Su, X. Y. , & Yau, H. T. . (2020). An automatic intelligent diagnostic mechanism for the milling cutter wear. *IEEE Access*, *8*, 199359-199368.

Ghasempoor A., Jeswiet, J., & Moore, T. N. (1999). Real time implementation of on-line tool condition monitoring in turning. *International Journal of Machine Tools and Manufacture*, *39*(12), 1883-1902.

Hesser, D. F., & Markert, B. (2019). Tool wear monitoring of a retrofitted CNC milling machine using artificial neural networks. *Manufacturing letters*, *19*, 1-4.

Kaya, B., Oysu, C., & Ertunc, H. M. (2011). Force-torque based on-line tool wear estimation system for CNC milling of Inconel 718 using neural networks. *Advances in Engineering Software*, *42*(3), 76-84.

Gomes, M. C., Brito, L. C., da Silva, M. B., & Duarte, M. A. V. (2021). Tool wear monitoring in micromilling using Support Vector Machine with vibration and sound sensors. *Precision Engineering*, *67*, 137-151.

Chungchoo, C., & Saini, D. (2002). On-line tool wear estimation in CNC turning operations using fuzzy neural network model. *International Journal of Machine Tools and Manufacture*, *42*(1), 29-40.

Li, W., & Liu, T. (2019). Time varying and condition adaptive hidden Markov model for tool wear state estimation and remaining useful life prediction in micro-milling. *Mechanical Systems and Signal Processing*, *131*, 689-702.

Li, C. B. . (2007). Acoustic emission method for tool condition monitoring based on wavelet analysis. The International Journal of Advanced Manufacturing Technology.

Li, X., Lim, B. S., Zhou, J. H., Huang, S., Phua, S. J., Shaw, K. C., & Er, M. J. (2009). Fuzzy neural network modelling for tool wear estimation in dry milling operation. In *Annual Conference of the PHM Society* (Vol. 1, No. 1).

Lv, Shuran, and, Lv, & Shujin. (2011). Applying bp neural network model to forecast peak velocity of blasting ground vibration. *Procedia Engineering*, *26*(1), 257-263.

Cai Shida is currently studying for a master 's degree in electronic information at Shenyang Jianzhu University in Shenyang, China. He earned a bachelor 's degree in automation in 2019. His main research direction is milling cutter wear prediction.

Sun Liangliang received his PhD degree in Control Theory and Control Engineering from Northeastern University, China, in 2015. He is currently a Professor of Information and Control Engineering at Shenyang Jianzhu University. His current research interests include Intelligent Manufacturing Systems, planning, scheduling, and coordination of design, manufacturing.

Mantong Zhao studied in the School of Economics and Management of Shenyang Institute of Technology. Her current research interests include Intelligent Manufacturing Systems, planning, scheduling, and coordination of design, manufacturing.

Wang Yue received her master's degree in Physical education and training from Beijing Sport University in 2012. He is now a lecturer in Sports Department of Shenyang Jianzhu University. Her current research interests include vocational education, higher education etc.

Li Xi was born in 1988 as a senior engineer with a master's degree. Her current research interests include Intelligent Manufacturing Systems, planning, scheduling, and coordination of design, manufacturing.

Peng Jiayu graduated from Shenyang Jianzhu University with bachelor's degree and master's degree, and is studying for doctor's degree in Shenyang Jianzhu University